# Huygens Titan Probe Trajectory Reconstruction Using Traditional Methods and the Program to Optimize Simulated Trajectories II

Scott A. Striepe, NASA Langley Research Center, Hampton, VA
Robert C. Blanchard, National Institute for Aerospace, Hampton, VA
Michael F. Kirsch, National Institute for Aerospace, Hampton, VA
Wallace T. Fowler, The University of Texas at Austin, Austin, TX

## Abstract

On January 14, 2005, ESA's Huygens probe separated from NASA's Cassini spacecraft, entered the Titan atmosphere and landed on its surface. As part of NASA Engineering Safety Center Independent Technical Assessment of the Huygens entry, descent, and landing, and an agreement with ESA, NASA provided results of all EDL analyses and associated findings to the Huygens project team prior to probe entry. In return, NASA was provided the flight data from the probe so that trajectory reconstruction could be done and simulation models assessed. Trajectory reconstruction of the Huygens entry probe at Titan was accomplished using two independent approaches: a traditional method and a POST2-based method. Results from both approaches are discussed in this paper.

## INTRODUCTION

On January 14, 2005, the European Space Agency's (ESA) Huygens probe separated from NASA's Cassini spacecraft, entered the Titan atmosphere and landed on its surface.[1-3] This probe used a multiple parachute system to enable atmospheric measurements to be recorded during the probe's over two hour descent to the surface. Digital images, radar altimetry, accelerometer data, and Earth-based radio telescope observations were also gathered during the entry, descent, and landing (EDL).[4-9] Figure 1 illustrates the Huygens probe's EDL profile. After atmospheric interface at 1270 km above the surface, the probe decelerates to around Mach 1.5 at pilot parachute deploy. This deploy event (designated T0) is triggered by a sequence of time and acceleration conditions and is the epoch time for all subsequent events and most data sets generated during the parachute descent phase. Three parachutes were used in the Huygens probe system: (1) a 2.5-sec Pilot parachute; (2) a 15-minute Main parachute; and (3) a 2.5-hour Drogue parachute. Data taken during the descent was relayed through the Cassini spacecraft as it flew by Titan.
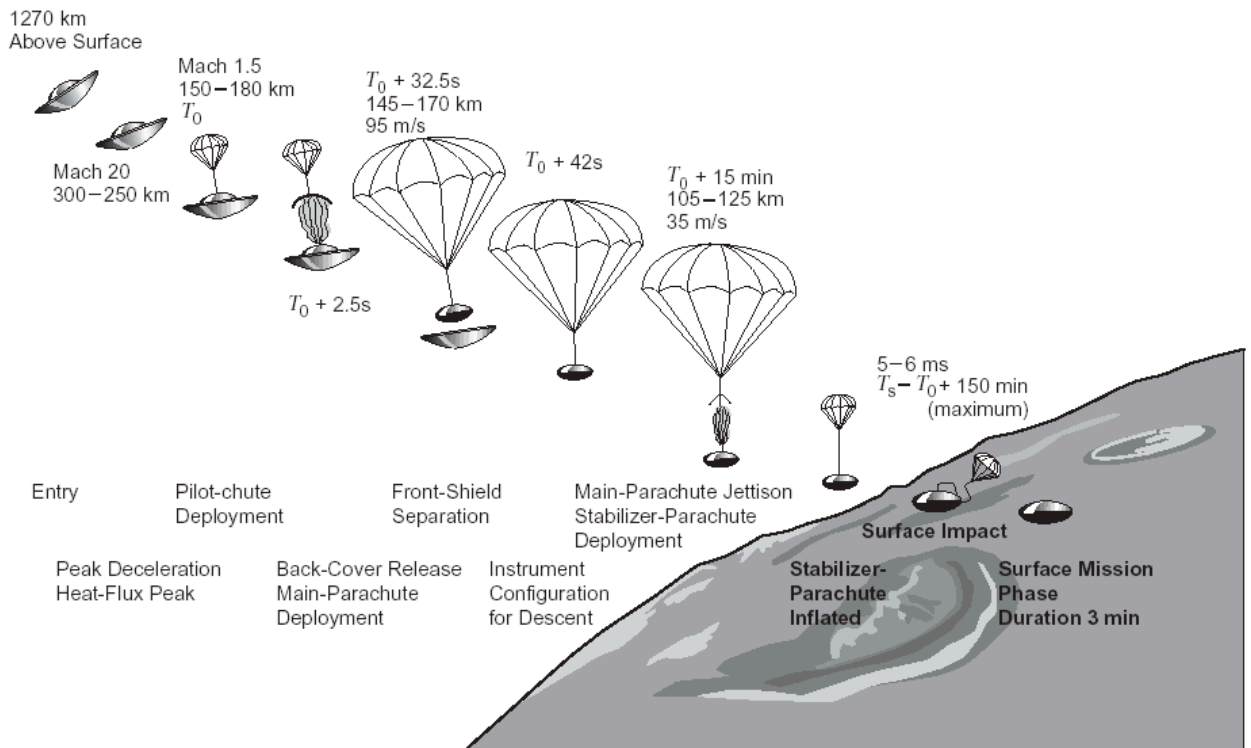
---

Figure 1. Huygens Titan probe Entry, Descent, and Landing Sequence[2]

NASA Langley was involved in the pre-entry EDL analyses of the Huygens probe. Analyses were conducted under the auspices of the NASA Engineering Safety Center's (NESC) Independent Technical Assessment (ITA) of the Cassini/Huygens probe EDL at Titan.[10] A Program to Optimize Simulated Trajectories II[11] (POST2)-based trajectory simulation was developed that included models of the probe aerodynamics, parachute trigger logic and drag models for the Pilot, Main, and Drogue parachutes. As part of the agreement with ESA, NASA provided results of all analyses and presented findings to both the Cassini and Huygens project teams. In return, NASA was provided the flight data from the probe so that trajectory reconstruction could be done and simulation models assessed. NASA has completed similar assessments of flight data to improve simulation models (such as capsule aerodynamics, parachute aerodynamics, and atmospheric density and winds) for the Mars Pathfinder EDL, Mars Odyssey aerobraking, and Mars Exploration Rovers EDL.[12-14] ESA had a team that provided the official project reconstruction of the Huygens EDL trajectory (the Huygens Descent Trajectory Working Group, or DTWG).[3] The main objective of this NESC sponsored activity was to reconstruct the Huygens Probe data to improve NASA's aerodynamics, atmospheric density and winds, and parachute performance models. The NASA NESC ITA team also analyzed the flight data to provide an independent trajectory reconstruction. The results of these analyses were provided to the DTWG and the Huygens Data Analysis Working Group (DAWG), with interaction between NASA, DTWG, and DAWG to discuss any differences in the reconstructed trajectory.

## BACKGROUND

Trajectory reconstruction of the Huygens entry probe at Titan was accomplished using two independent approaches. One was a traditional approach to trajectory reconstruction that integrates the accelerometer measurements directly during the entry phase (forward) and integrates the hydrostatic equation using the temperature and pressure measurements to determine altitude and velocity (backwards). The other approach used a Kalman filter module developed for reconstruction in conjunction with the POST2-based simulation. The POST2-based reconstruction uses accelerometer measurements to adjust an estimated state using a POST2-based simulation developed prior to entry to support EDL analyses and design. Results from both approaches are discussed in this paper.

The ESA Huygens probe science teams provided several sets of data. These data included acceleration measurements throughout EDL, pressure and temperature after heatshield jettison, and radar altimetry for the last 40 kilometers. Additionally, radio telescopes at Earth received the Huygens signal throughout the descent and provided an estimate of wind velocity. The Descent Imager (DI) team also contributed an estimate of vertical velocity based on sequentially captured images.

The main emphasis of the Huygens probe reconstruction is to evaluate the simulation models used prior to probe entry at Titan with actual flight data. Another objective of the Huygens reconstruction was to compare the NASA derived trajectory and the Huygens DTWG solution to the trajectory profile.

## RECONSTRUCTION APPROACHS

### *Traditional Method*

Using the traditional method, the trajectory reconstruction of the Huygens probe trajectory parameters from entry interface to the surface of Titian is separated into two parts. First, the probe trajectory on the Drogue parachute (lasting about 8650 s) is addressed. Next the probe entry phase trajectory (the main deceleration pulse), leading to the parachute phase and culminating just prior to the Drogue deploy (lasting about 350 s) is reconstructed.

The reconstruction of the trajectory during the Drogue phase of the Huygens probe descent to the surface is obtained using the pressure, temperature, and acceleration data. In essence, the method involves integrating a form of the hydrostatic equation to obtain altitude, and applying the aerodynamic force equation to get total relative velocity magnitude. This approach is taken to circumvent the problems associated with integrating the accelerometer data during long time intervals at near terminal velocity conditions.

The second half of the reconstruction was done in a more classical sense. It involved the hypersonic portion of the flight starting from entry interface. By using the acceleration data along with the navigation team provided state at entry interface the trajectory was reconstructed by integrating the accelerations. After the trajectory was reconstructed the atmosphere could be backed out using the aerodynamic database.

Atmosphere Reconstruction

The accelerometer data from an entry probe during descent is the principle data used to obtain the free-stream density. The aerodynamic force equation along the x-body axis can be expressed as,

$$\rho = \frac{2ma_x}{v_r^2 C_A S}$$

where the probe mass, m, reference area, S, and the axial aerodynamic force coefficient, $C_A$ are known a priori, and $v_r$ is the probe velocity relative to the atmosphere. Given the reconstruction trajectory state variables (i.e. probe position, velocity, and orientation as a function of time); density mapping is relatively straight forward, except for the $C_A$, which is also a function of density (along with other parameters). This transcendental nature of the density equation above can be overcome by a simple iterative technique.

The aerodynamic coefficient for the hypersonic phase, $C_A$, is determined using the preflight database created by NASA Langley. This database requires the current values for the center-of-gravity location, Knudsen number, Mach number, relative velocity; angle of attack and sideslip angle are assumed zero. During the parachute/drogue phase, the composite $C_A S$ coefficient is determined as a linear combination of probe and parachute drag. That is, for the total $C_A S$ term the product of the approximate drag coefficient, $C_D$ (.8) and the heat shield reference area (5.73), or the descent module reference area (1.29) was added to the parachute drag (a function of Mach Number and Reynolds Number) times its reference area.

Drogue-Phase Equations of Motion (Hydrostatic equation)

The equation for the change in pressure due to a change in altitude of a fluid, such as an atmosphere, is known as the hydrostatic equation, and is given as:

$$\frac{dp}{dh} = -g\rho \tag{1}$$

Using the chain rule, substituting in equation (1) and solving for the altitude time derivative gives:

$$\frac{dh}{dt} = \frac{\dot{p}}{-g\rho} \tag{2}$$

Putting the density (from the equation of state using the measured temperature and pressure) and gravity into equation 2, gives a transcendental equation that is a function of the measured quantities that can be evaluated and integrated to get the vertical velocity component and the altitude time history.

$$\frac{dh}{dt} = \frac{R(R_o + h)^2 T}{-\mu C_f W_{MM}} \left( \frac{\dot{p}}{p} \right) \tag{3}$$

This equation is integrated using the Ordinary Differential Equation (ODE) solver that is built into MatLab. It requires that the pressure, temperature, mean molecular weight, and pressure derivative be given as a function of time. The gravity and compression factor are functions of altitude but since an ODE solver is being used, which uses the previous time point to calculate the derivative to get to the next point, the altitude is known. Since the time of surface impact is known, the integration is done from the surface up. In summary, from the measurements of pressure and temperature as a function of time, two of the six trajectory state variables ($h$, $\dot{h}$) as a function of time are obtained.

*POST2-based Method*

A six degree-of-freedom atmospheric entry and three degree-of-freedom parachute descent trajectory of the Huygens probe was simulated in Program to Optimize Simulated Trajectories II (POST2).[11] POST2 is a generalized point mass, discrete parameter targeting and optimization trajectory program. POST2 has the ability to simulate three and six degree-of-freedom (3DOF and 6DOF) trajectories for multiple vehicles in various flight regimes. POST2 also has the capability to include different atmosphere, aerodynamics, gravity, propulsion, parachute and navigation system models. Many of these models have been used to simulate the entry trajectories for previous missions (i.e., MER, Genesis, Mars Pathfinder)[15-17] as well as current and planned NASA missions (Stardust, Mars Phoenix, and Mars Science Laboratory).[18,19] A variety of system studies have been conducted and their atmospheric trajectories simulated in POST2 including aerocapture at Titan, Neptune and Venus.[20]

Exploiting the modular nature of the POST2 program by adding mission specific models in concert with the existing POST2 architecture allows for the development of higher fidelity, mission specific simulations. These simulations usually have integrated mission-specific engineering models and flight software that have been tested and validated prior to the actual mission. These simulations support design, development, testing, and operations of vehicles for particular missions. These POST2-based mission specific simulations have been used operationally for day-of-entry flight software parameter determination and prediction of mission metrics (such as touchdown footprint) as well as aerobraking orbit prediction and assessment. Simulation complexity varies from first-order trades (e.g. parachute size and deployment conditions, terminal descent engine size, etc.) to all-up Monte-Carlo simulations for flight operations.

POST2 was used to simulate the Huygens entry trajectory into Titan.[10] The POST2-based flight simulation incorporated several models specific to the Huygens probe entry: a 6DOF aerodynamics model; Titan's gravity and Titan-GRAM atmosphere (including wind) models; attitude inputs and initial states; trigger criteria, inflation, and drag models for the Pilot, Main, and Drogue parachutes; as well as vehicle geometric parameters. Note that version 1.0 of the Titan-GRAM atmospheric model was implemented into POST2, with updates from Cassini measurements of Titan (the T0 and TA atmospheric profiles). This simulation was used to produce single trajectory data and was an integral element of the Monte Carlo analyses discussed in Ref. 10.

Extended Kalman Filter POST2 Module

        An extended Kalman filter (EKF) module has been developed for and included into POST2. This module was developed and integrated into the POST2 software to facilitate trajectory reconstruction using POST2-based mission specific simulations. The general nature of POST2 inputs was retained for this module. That is, the state to be estimated can be input as any POST2 input and the observation can be any POST2 outputs. While the general POST2 software architecture was retained, separate files of observations and their associated weightings versus simulation time are required for use with this EKF module. The utility of integrating this EKF function into POST2 is to allow more rapid setup and execution of trajectory reconstruction runs using the same simulation that has been tested and validated for that particular mission.

        The theory and equations defining this module are well described in the literature.[21,22]  A summary of the method implemented for the POST2 module is as follows:

1) Define initial covariance and estimated state ($P_0$ and $X_0$)
2) Read observations (O) and their weights ($W = R^{-1}$) from files
3) Integrate to the next observation time:

$$\dot{X} = F(X,t) \text{ and } \qquad \dot{\overline{P}} = A*\overline{P} + \overline{P}*A^T + Q - K*R*K^T$$

where $\overline{P}$ is the propagated state covariance matrix; A is the matrix of state derivative with respect to time ($\dot{X}$) sensitivity to the state ($\frac{\partial \dot{X}}{\partial X}$); Q is the system noise covariance matrix (where the random noise is chosen to apply to every state); matrix K is from the last update; and R (the measurement noise covariance) is set to the inverse of the observation weightings matrix (W).

4)   At the observation time, calculate:

$$Y = O - G \qquad\qquad H = \frac{\partial G}{\partial X} \qquad\qquad K = \overline{P}*H^T*(H*\overline{P}*H^T - R)^{-1}$$

where O is the observation matrix (from file), G is the matrix of calculated observation values from the simulation and K is the Kalman gain.

5) Next update the state:
$$\hat{X} = \overline{X} + K*Y$$

6) And update the covariance:

$$\hat{P} = (I - K*H)*\overline{P}*(I - K*H)^T + K*R*K^T$$

where I is the identity matrix, $\hat{X}$ is the estimated state, and $\hat{P}$ is the updated covariance. This process is continued with POST2 integrating the state and covariance between observation updates.

**Huygens EDL Measured Datasets**

The Huygens entry, descent, and landing datasets described below were provided to NASA as part of an agreement with ESA for analyses NASA performed prior to entry. These datasets include measurements of atmospheric pressure, temperature, composition, and zonal winds, vehicle acceleration, and vehicle altitude. Various Principal Investigators were responsible for the instruments that provided this data; the various groups responsible for this data are identified, along with details about their instruments, in Refs. 1 and 2.

*Pressure*

The time history of the reduced pressure was obtained from ESA as described above. Figure 2 (top panel) shows the free-stream pressure from the onboard pressure transducer as a function of time where the reference time is entry interface. (During the day of entry, Jan. 14, 2005, $t_{EI}$ = 09:05:52.523)
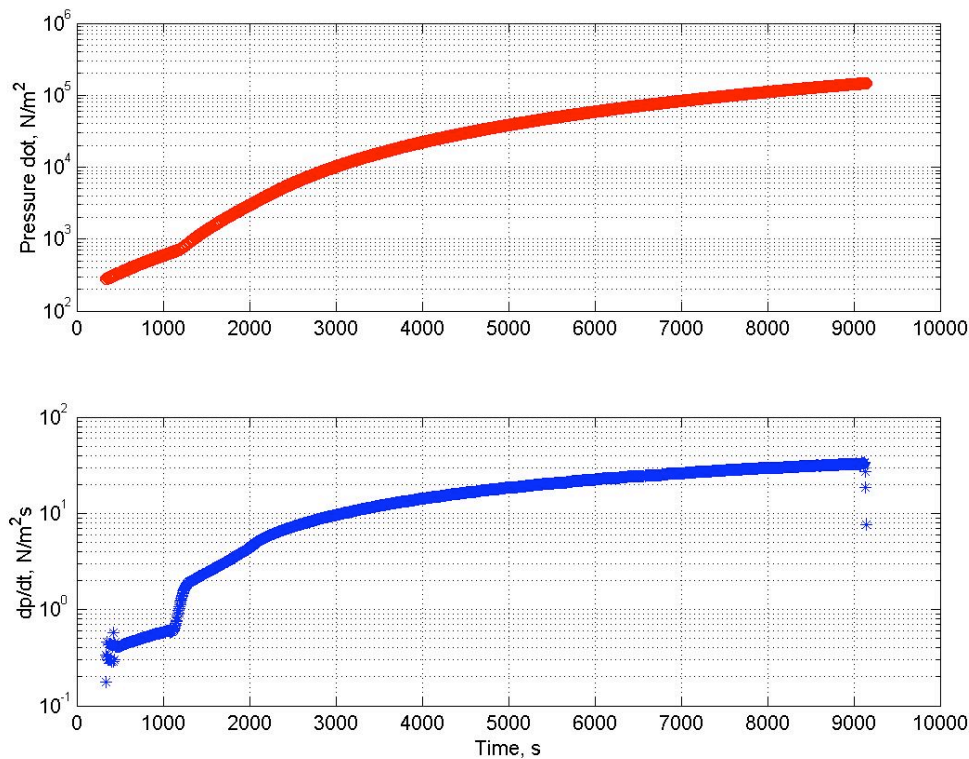


Figure 2: *Upper Panel*: Free-stream pressure provided by ESA.
*Lower Panel*: Pressure derivative using a 51-point sliding window with a third degree polynomial evaluated at the mid-point.

Derivative of Pressure

The time derivative of pressure is needed for the calculation of altitude, see equation (3). The method used to obtain the pressure derivative includes fitting a third degree polynomial (using least-squares) to a 51-point sliding window of pressure data. That is, at any time point, 25 pressure data to the left and right are fitted to a $3^{rd}$-degree polynomial from which a derivative in obtained for the time point. One point to the right

is added, while one point to the left is dropped from the original data set and the process is repeated. This method clearly leaves 25 points at the beginning and at the end of the data set without a derivative. To handle these end points, the window size is reduced to 5 points, leaving only two points without a derivative. Figure 2 (lower panel) shows the results of the calculations for the time derivative of pressure, dp/dt. The derivative is relatively smooth except at the end data points, as expected. The left end of the graph has a little extra noise providing a few points with an unreliable derivative. On the ground, the derivative goes to zero and this "corner" impacts the last few derivatives, as seen in the graph. Neither end produces difficulty in the integration process since the points can be readily omitted.

*Density*

The density is obtained from the calibrated measurements of pressure and temperature using the equation of state. In addition, the mean molecular weight and the compression factor (also taken from data provided through ESA, but not shown here) are used in the calculation of density. Figure 3 shows the density results for both with and without (Cf=1) compression factor. As expected, the difference is less than 3.5% and the larger differences occur at lower altitudes, corresponding to larger values of time, as shown in Fig. 3.
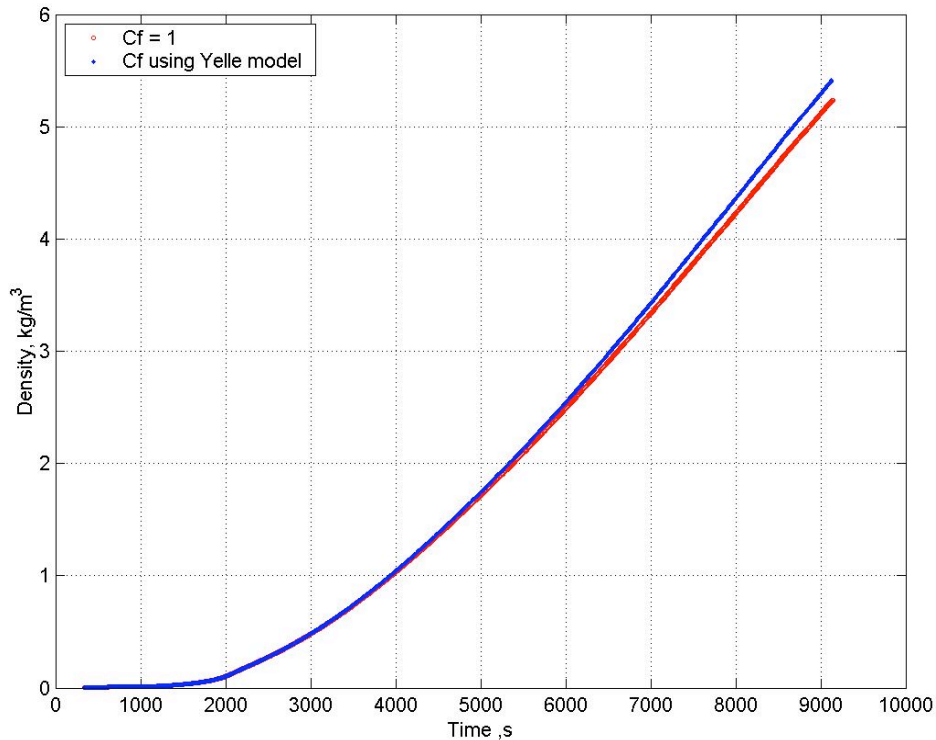


Figure 3: Density time history with and without compression effects.

*Altimeter*

Two separate independent altimeters, labeled "A" and "B", were onboard the Huygens probe. Figure 4 shows the data for both of these instruments after the Principal Investigator has applied calibration factors. The data produced by both altimeter

instruments lay on top of one another, although the altimeter B data starts at a higher altitude.
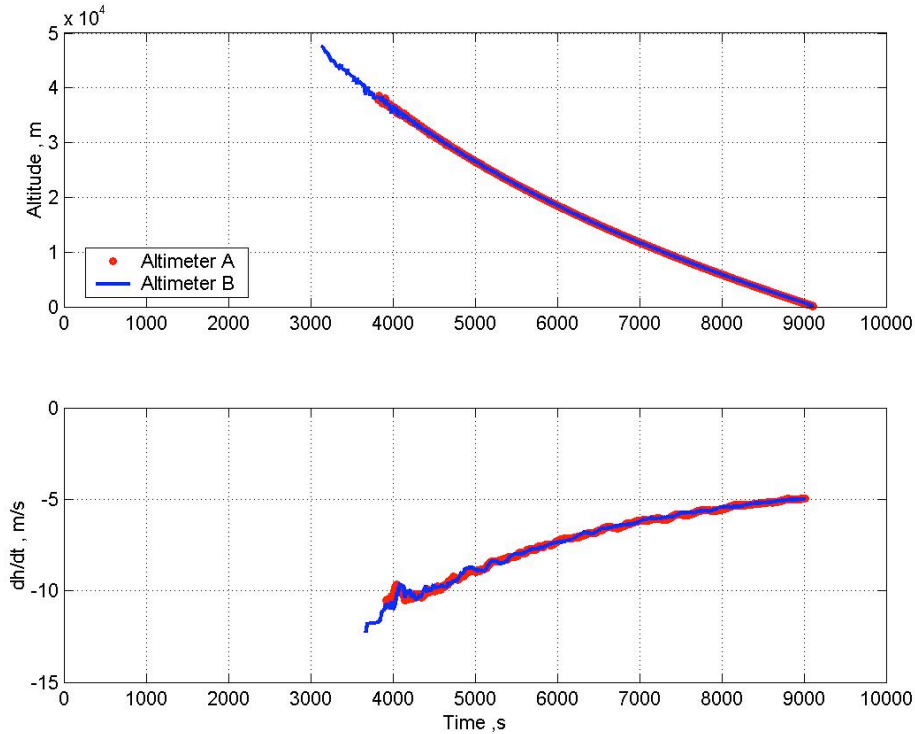


Figure 4: *Top Panel*: Altimeter measurements from A and B instruments.
*Lower Panel*: Derivative of altimeter data using a 101-point moving window.

*Accelerometer*

The axial acceleration data set from the Huygens Servo Accelerometer, used in the reconstruction is shown in Fig. 5. Note that Piezo Accelerometer data in all three axes were received, but evaluation of this dataset deemed it unusable (the axial component only reached 100 m/s$^2$, well below the values expected and returned from two independent sources, and forcing the lateral measurements to be rejected as well). Examination of the Servo axial accelerometer data before entry interface indicated that there is a bias in the data of about 22.8 μ-g in the data. In Fig. 5 the top panel shows the data from entry interface to near probe touchdown on the surface of Titan. The lower panel shows an expanded view of the data. In this panel the results of a smoothing process is shown along with the original data. Smoothing was done on data beyond 330 s, or right after parachute inflation. The smoothing process consists of a median process for a sliding window, similar to what was done for the calculation of dp/dt and dh/dt, discussed earlier, except a median is obtained instead of a curve fit. That is, a window size of 201 data points is selected and a median of the data set is determined. The time and median value are recorded at the middle of the data and subsequently, a data point is added to the right and one deleted to the left and the process is repeated. Again, because of the moving window the first and last 100 points of data in the original data set remain not smoothed. The first 100 points are used to merge with the original data set, while the last 100 points are not smoothed, as can be seen in Fig. 5. The spike in the acceleration data at approximately 1100 seconds corresponds to drogue deploy which represents real

data and as such the peak must be preserved so as to not lose the information. Thus, in this time interval smoothing was not attempted. Similarly, the hypersonic portion of the acceleration time history before main parachute deploy, i.e. before approximately 330 seconds, is also not smoothed so as not to lose the peak acceleration data. In summary, the blue line in Fig. 5 represents the acceleration data used in the calculations reported in the next sections.
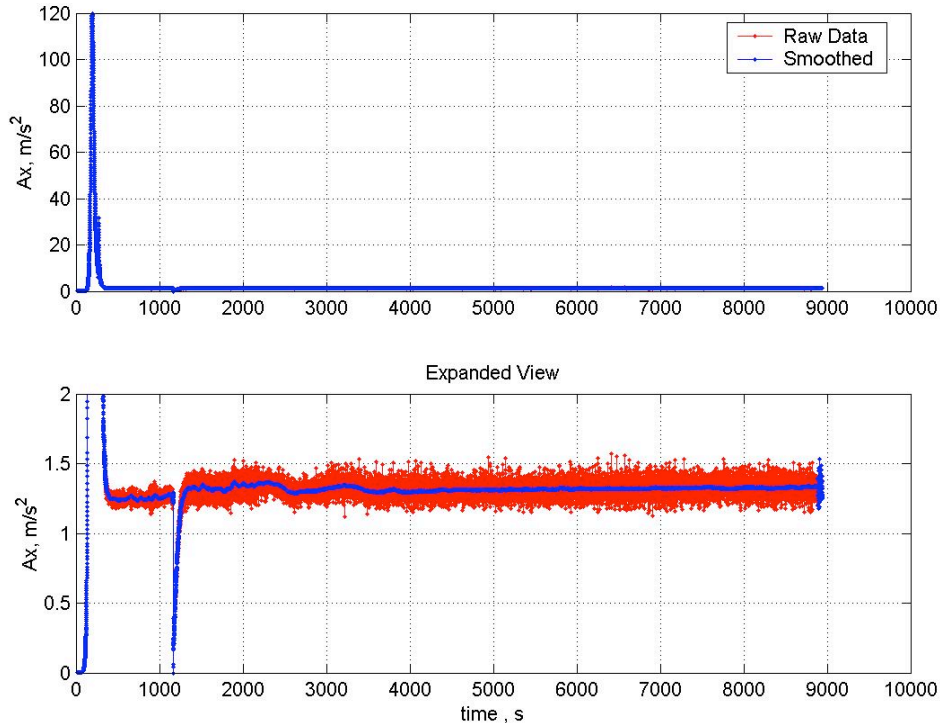


Figure 5: *Upper Panel:* Huygens axial accel from Entry Interface to Titan's surface. *Lower Panel:* Expanded view of axial acceleration showing smooth and actual accel data.

## RESULTS

*Traditional Method*

Figures 6, 7, and 8 show the atmosphere results for the hypersonic reentry phase of the mission (denoted "Hyper" in the legend), namely density, pressure, and temperature as a function of altitude, respectively. Included on each graph is the Huygens model atmosphere generated by Yelle and the Titan-GRAM Atmosphere used in simulations. Also included in the figures is the lower atmosphere reconstructed density using the equation of state (denoted "Hydro" in the legend) as well as the measured pressures and temperatures.
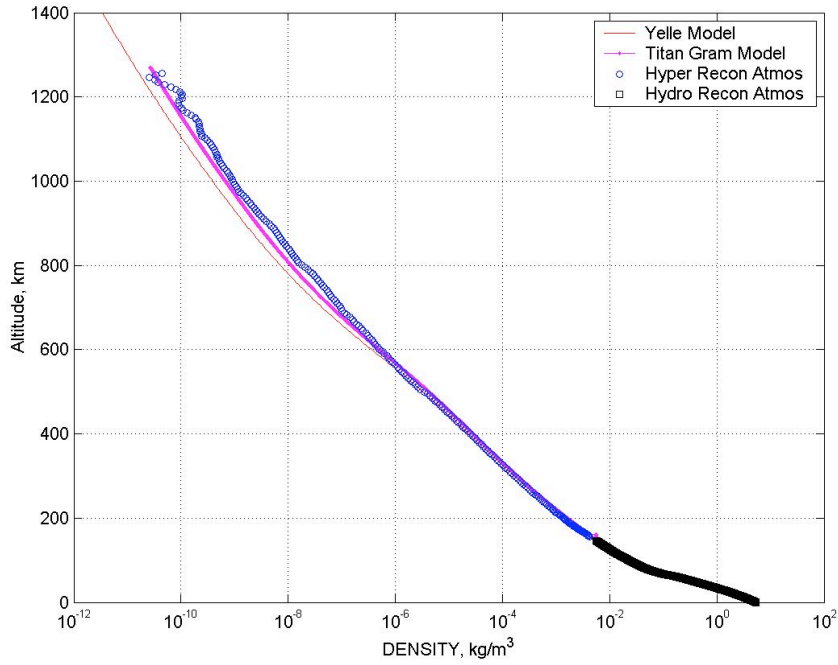
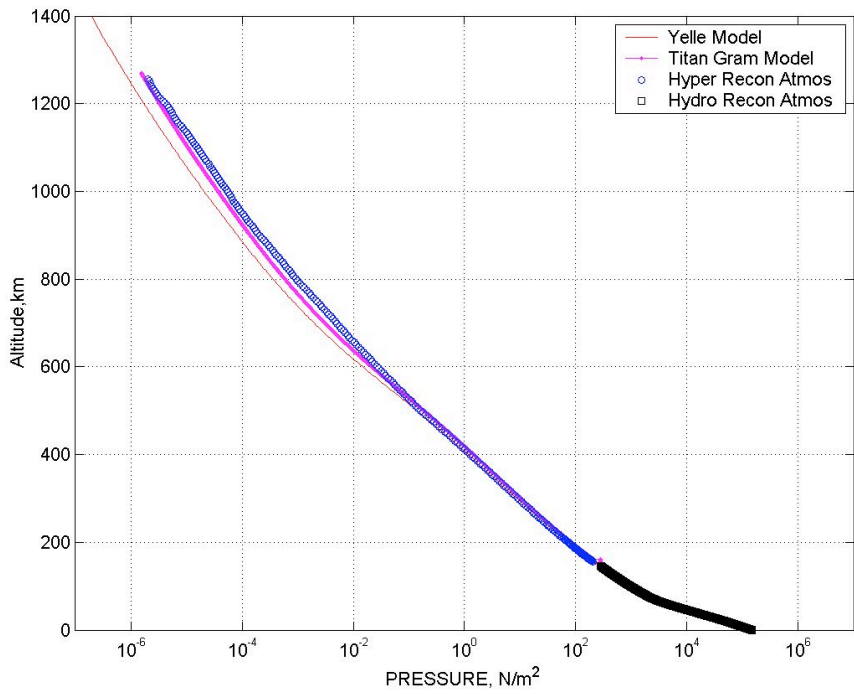Figure 6: Reconstructed atmospheric density as a function of altitude.



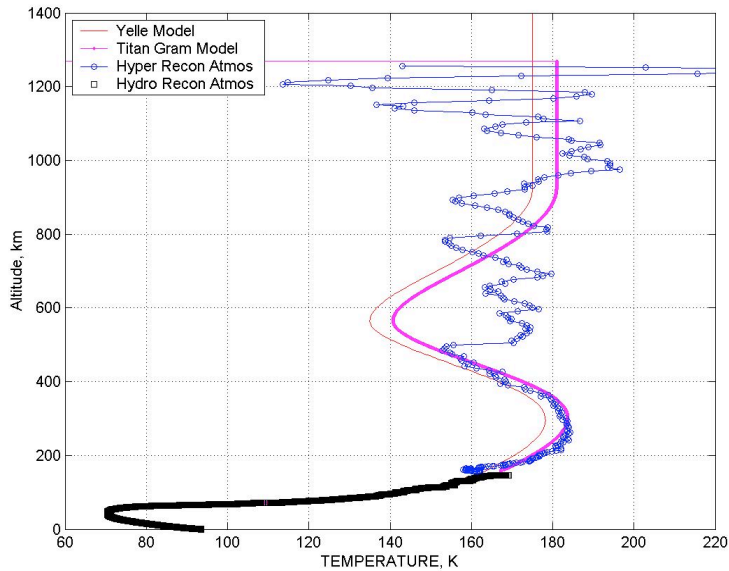Figure 7: Reconstructed atmospheric pressure as a function of altitude.

Figure 8: Reconstructed atmospheric temperature as a function of altitude.

The atmosphere state (density, pressure, and temperature) graphs also include the lower altitude measurement data discussed earlier for completeness. At the lower altitude (approximately less than 500 km) there is an excellent match between the Yelle model and the measurements, and an even better match with the Titan-GRAM. At altitudes larger than about 500 km, both the density and pressure give higher values at the exosphere base resulting in temperature that agrees with the model. Between about 500 and 800 km, the model appears to diverge slightly, resulting in temperature differences of only about 30 K. For the entire atmosphere profile the Titan-GRAM model agrees more closely to the reconstruction than the Yelle model. To facilitate the comparison of the reconstructed density to the models a comparison chart showing the percent difference between the reconstruction and the model was created and is presented as Fig. 9.
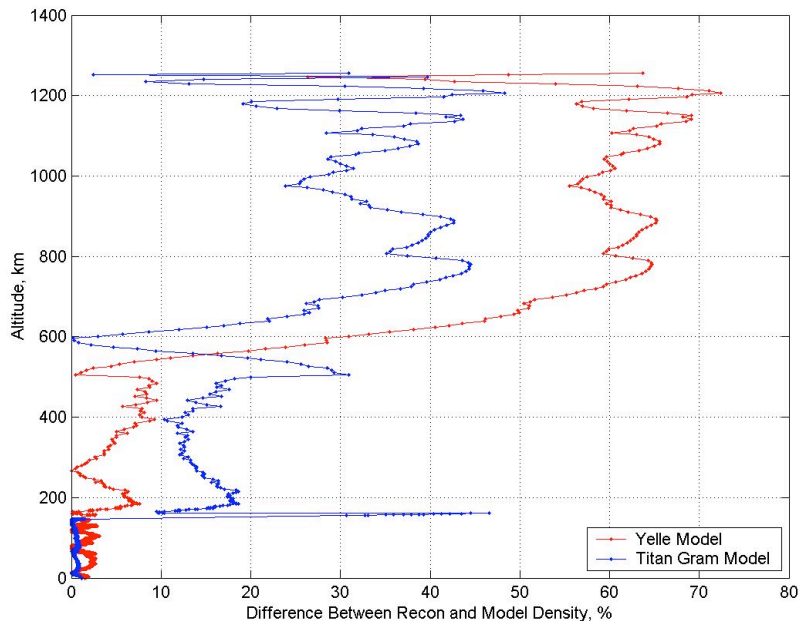


Figure 9: Percent Difference Between Reconstructed Density and Model Densities

Drogue Trajectory Reconstruction

Figure 10 shows the altitude results from the integration of equation (3) starting at the ground and ending near the time when the heat shield is jettisoned. The change in the slope of altitude after about 1100 s shown in the graph is the drogue deployment. Included on the graph are both of the altimeter measurements taken at altitudes starting at about 40 km.
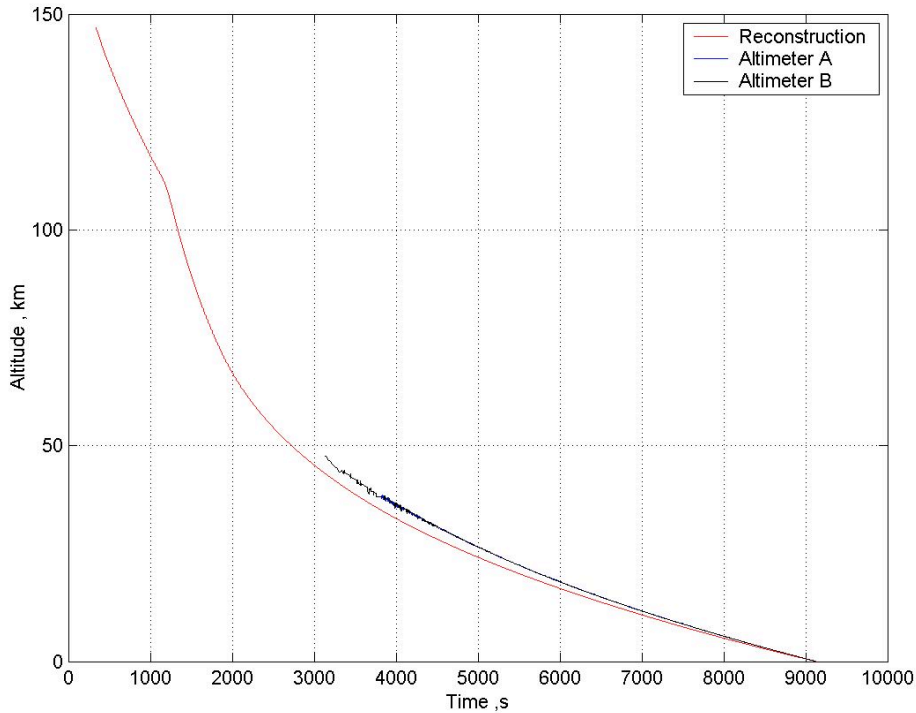


Figure 10: Reconstructed altitude compared to both altimeter measurements.

Figure 11 shows a more detailed comparison between the reconstructed altitude and the altimeter-A measurements (as mentioned above, both altimeters-A and B provided nearly the same data, so only altimeter-A will be shown). In addition, the corresponding residuals are plotted to show the detail differences. Clearly, as seen in the lower panel for Fig. 11, there is a systematic difference between the reconstructed altitude and the altimeter measurements for this altimeter (the same differences of about the same magnitude apply to altimeter-B).
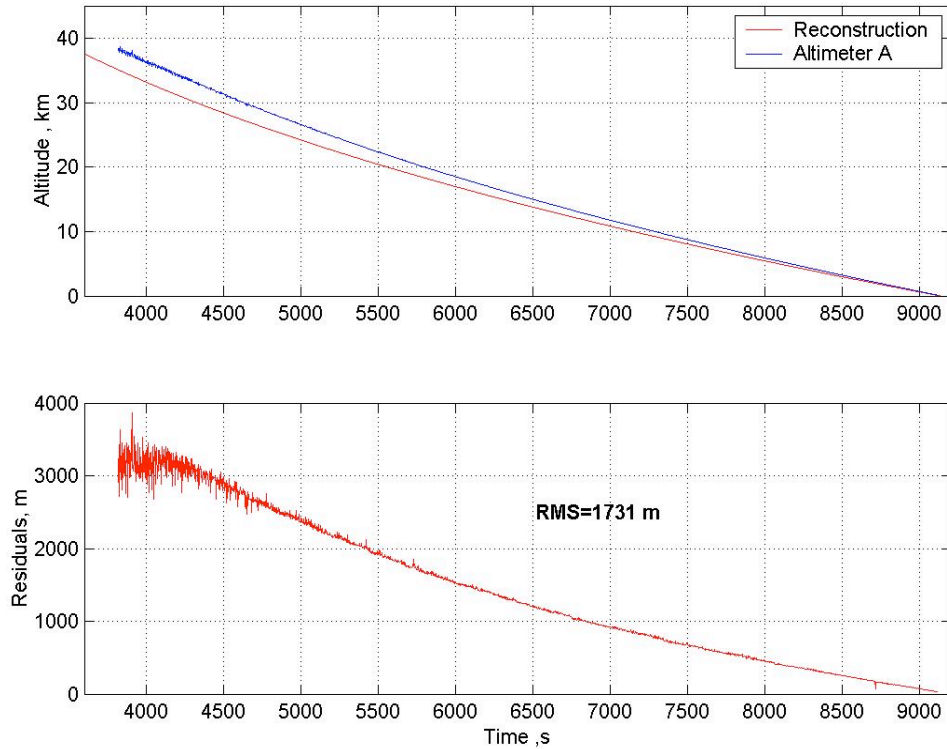
Figure 11: *Upper Panel*: Altimeter A comparison to the reconstructed altitude.
*Lower Panel*: Altitude measurement residuals with the RMS.

Descent Phase Comparisons

Figure 12 shows a comparison of the reconstructed altitudes obtained by the DTWG with the altitudes developed using other reconstruction methods. There is excellent agreement with the DTWG reconstructed altitudes using the traditional reconstruction method described in this report (the POST2-based method results are discussed in following sections). The two curves lie almost on top of each other (about 300 m difference at the upper altitudes to about 10 m near the surface). This result is mainly due to the similarity in reconstructed methods. Namely, the DTWG method uses an approximate integral, while numerical integration is used herein. Clearly, the DTWG method does not match the altimetry measurements.
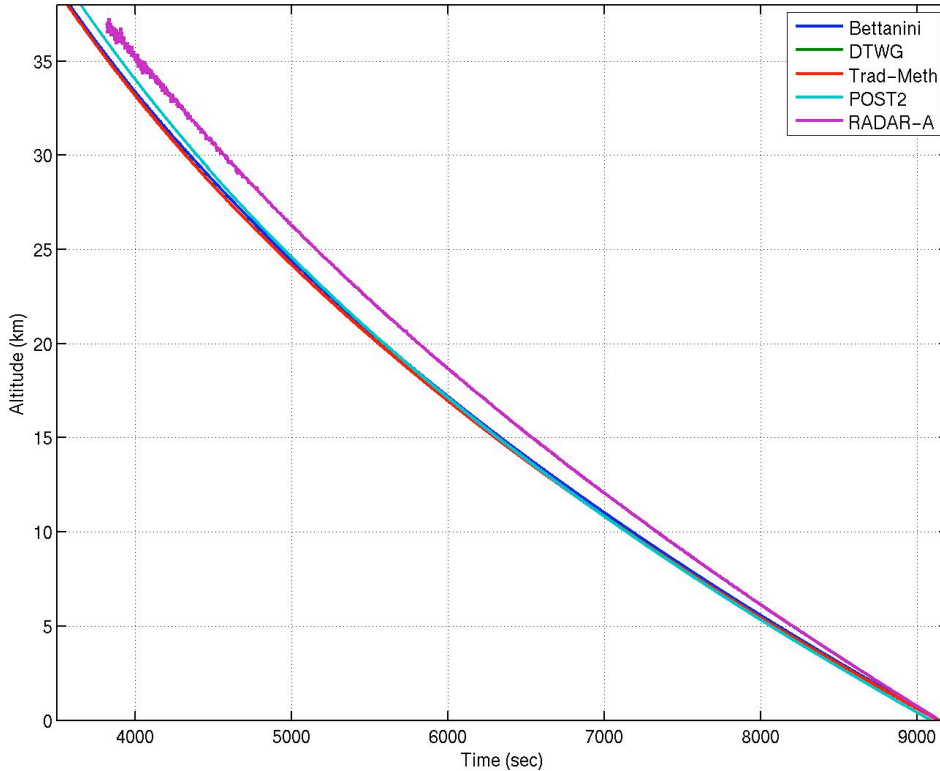
Figure 12: Reconstructed altitude comparison with RADAR

Figure 12 also shows a similar comparison of the reconstructed altitudes obtained by Carlo Bettanini, a member of the Huygens Atmospheric Structure Instrument team (personal communication, 20 September 2006). There is good agreement between these results also. Once again the reconstruction does not match the radar altimetry data; note that Bettanini's method does not use the altimetry measurements to reconstruct altitude. His method relies upon integration of the pressure measurements combined with accelerometer data from the ground upward. There are differences at higher altitudes (above 105 km) where Bettanini altitudes are lower in value than what is generated using the methods in this report. In summary, the altitude results using the traditional method match the DTWG and Bettanini reconstructed altitudes. However, when compared to the radar altimetry data, a systematic error is readily evident. One possible solution is to introduce a scale factor on the radar altimetry data.

Altitude Error Bound Estimation
        A useful metric for understanding the altitude variation is to estimate the error in the altitude reconstruction, i.e. determine error bars or bounds. Since the altitude is found by integrating the measured data it stands to reason that a main source of uncertainty in the altitude would come from the uncertainty in the measurements. The measurements of the pressure, temperature, and mean molecular weight each have their own associated uncertainty. To find the extent of the error bounds for velocity the two extreme cases of measurement uncertainty were taken, that is all were either high or low. That is, changing each measurement by adding its uncertainty to it for the high case and subtracting for the low case. After adjusting the measurement, the integration was done again to find the upper and lower bounds of the error bar on altitude. Because of the large scale of the

altitude, 0 to 150 km, the error bars are difficult to visualize. Therefore it is easier to show the size of the error bounds as a function of altitude rather than the actual bounds on either side of the altitude history. This error is shown in Fig. 13, where it can be seen that the error bounds are relatively small in comparison to the actual altitude.
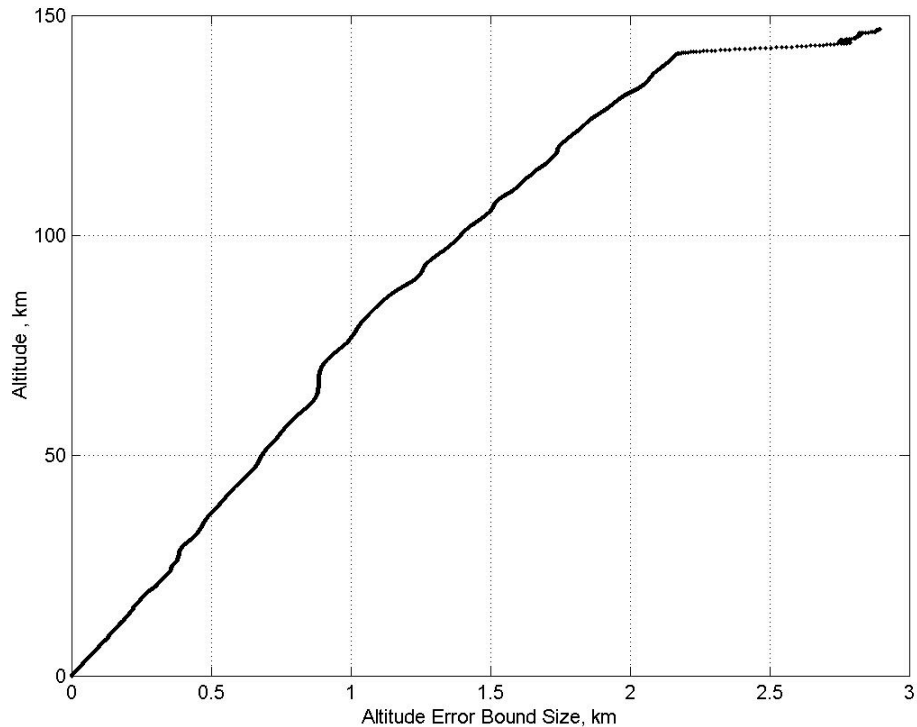


Figure 13: Altitude Error Bound Size as a function of Altitude

## *POST2-based Method*

The trajectory reconstruction runs using POST2 focused on estimating entry aerodynamics, parachute phase parameters, and the vehicle state (position and velocity) throughout the entire EDL trajectory. Although the simulation results using the JPL-determined last estimated nominal entry state generally follows the flight data, a Monte Carlo analysis was used to try to determine the initial state (inertial position and velocity vectors) that best fits the flight data through the entry phase (where the main deceleration pulse occurs). The last JPL delivered initial state covariance was used to generate 10000 dispersed states. Each case was simulated and the root sum square (RSS) was taken of the acceleration observation residual as the simulation progressed. The initial state from the smallest value cases was used for subsequent reconstruction efforts. Table 1 compares the nominal best estimated entry state generated by JPL (along with the 3-sigma bounds) and the initial state determined by the Monte Carlo process (and the differences between them). Note that all times in the following sections are from entry interface and not Pilot parachute deployment (or T0).

Table 1. Comparison of JPL Last Initial State Estimate and Monte Carlo Determined Initial State

|  | JPL last estimate | 3-σ bounds | Monte Carlo determined | Difference |
|---|---|---|---|---|
| Inertial X Position (km) | -3785.053 | 94.718 | -3810.021 | 24.968 |
| Inertial Y Position (km) | 366.623 | 24.508 | 367.226 | -0.603 |
| Inertial Z Position (km) | -568.429 | 10.214 | -566.418 | -2.011 |
| Inertial X Velocity (km/s) | 5.704492 | 0.009794 | 5.701933 | 0.002559 |
| Inertial X Velocity (km/s) | 1.918924 | 0.001877 | 1.918745 | 0.000179 |
| Inertial X Velocity (km/s) | 0.390306 | 0.001727 | 0.389695 | 0.000611 |

Entry Aerodynamics

The focus of this section is to validate the entry aerodynamics model from the pre-entry simulation using the flight data. For this portion of the analysis, the Titan-GRAM atmosphere model is assumed correct and all of the error in the measured accelerations is due to errors in the aerodynamics model. The POST2-based Huygens EDL simulation was setup to include aerodynamic uncertainties for Monte Carlo simulations done prior to probe arrival at Titan. The aerodynamic database includes the uncertainty amount for the free molecular, hypersonic and supersonic flight regimes. For the reconstruction analyses, the uncertainty in axial force coefficient was estimated since only the axial accelerations were measured. Note that these were entry phase runs only, hence no reconstructed trajectory data is generated beyond the Pilot parachute mortar firing event (aka T0 event) at about 270 sec.

As noted previously, the Kalman filter implementation includes system noise covariance input. Through the state covariance, this noise covariance can be used to increase the reconstructed state response to the measurements. The peak deceleration region during entry is shown for the reconstruction case with the noise covariance set for a rapid filter response to the measurements in Fig. 14. This "Low Noise" (or LN) setting allows an assessment of the entry aerodynamic model used prior to Huygens probe entry at Titan by assuming that all of the error during the entry is from aerodynamic misprediction; whereas a "High Noise" (or HN) setting does not allow the filter to change the estimate as rapidly. As seen in this figure, the acceleration for the LN case matched acceleration points closely as desired. The maximum error during this peak deceleration period was +/- 0.6 m/s$^2$ (or less than 0.5%); most of the error in this region was less than 0.2 m/s$^2$ (or 0.2%).
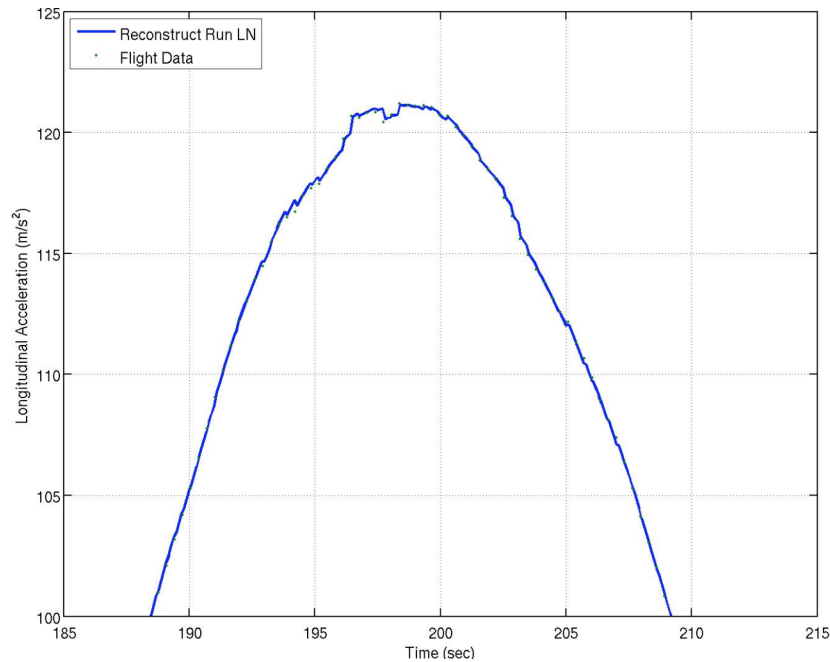
Figure 14. Comparison of Flight Data to Entry Aerodynamics Estimate Reconstruction Run – Peak Deceleration Region – Low Noise

These reconstruction runs were estimating the adjustment from the nominal aerodynamics model necessary to meet the flight data. The actual states estimated were the aerodynamic dispersion parameters for $C_A$ in each flight regime (free molecular, hypersonic and supersonic). These parameters varied between +/- 1 and applied the aerodynamicist-defined uncertainty to the coefficient in each regime. For example, in the free molecular flight regime an uncertainty parameter of +1 corresponds to a multiplier of 5% on $C_A$; that is, the nominal $C_A$ was multiplied by 1.05 for an uncertainty parameter of +1 in the free molecular flight regime.
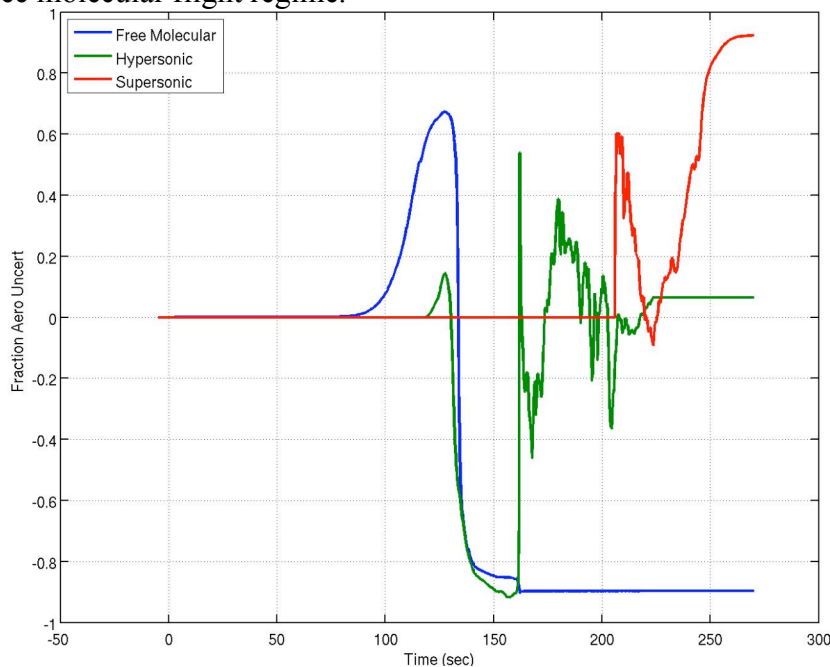


Figure 15 Estimated Entry Axial Force Aerodynamic Uncertainty Parameters -Low Noise

The estimated uncertainty parameters for the LN reconstruction case are shown in Fig. 15. Note that, the aerodynamics model allowed for overlap between the flight regimes, hence there are regions of the plot where two parameters are active at the same time. Otherwise, the unused uncertainty parameter is a constant value. The key result from this figure is the fact that even with all the error during entry attributed to the aerodynamics the estimated solution never exceeds the 3-sigma uncertainty bounds (never greater than +1 or less than -1) established by the aerodynamicists prior to entry. This significant result indicates that the entry aerodynamics model captured the aerodynamics of the Huygens entry capsule throughout all three flight regimes.
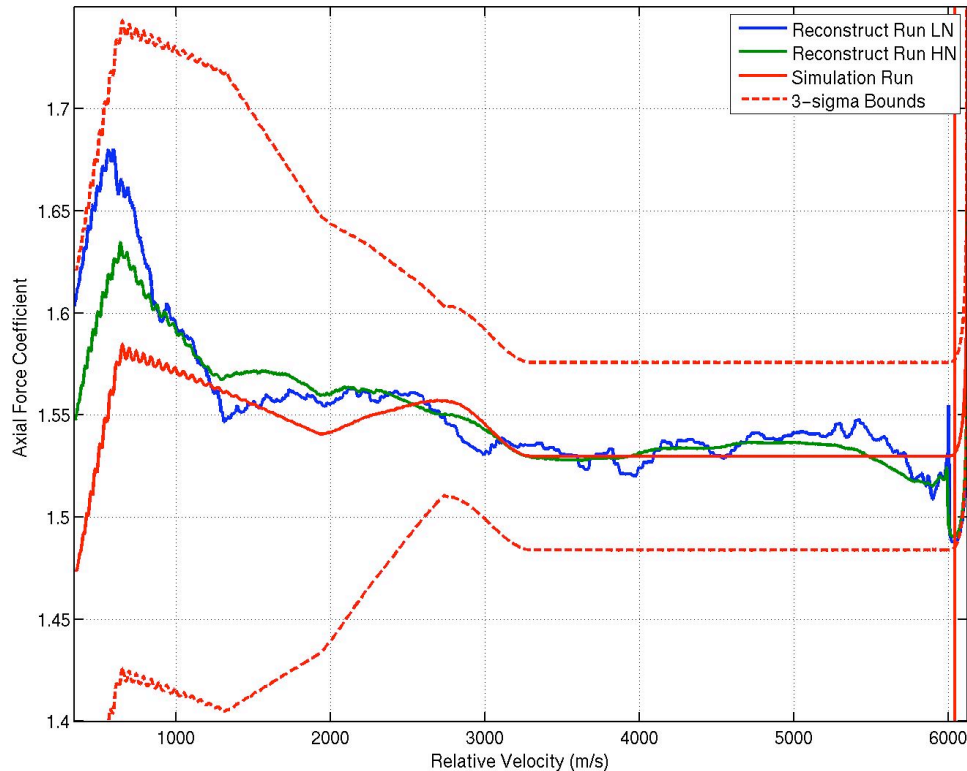


Figure 16 Estimated Entry Aerodynamic Axial Force Coefficient Values

Figure 16 shows the actual axial coefficient values corresponding to the estimated uncertainty parameters throughout entry for both the HN and LN versions of this reconstruction case as well as the simulation only case as a function of relative velocity. The 3-$\sigma$ axial force coefficient uncertainty bounds established before probe entry are also shown in the figure. Note that the even in the extreme case of assuming all errors are in the aerodynamics (the LN case) the axial force coefficient is within the pre-entry boundaries. As expected, the LN case has more variation in the axial coefficient than the HN case. Also, the HN results (which is closer to the nominal aerodynamics) are roughly the mean of the LN case as would also be expected since the HN case does not "chase" the measurement data points as rapidly as the LN case does. While a bit higher towards the end of the entry phase (around 1000 m/s), this reconstructed case shows little adjustment in $C_A$ is required beyond the nominal predicted values to be consistent with the flight data. This result again indicates that the pre-entry aerodynamics predictions

appear to have been accurate within the degree of uncertainty associated with the analysis.

Parachute Phase Assessment

For the entry phase, the dominant aerodynamic force is acting in the direction of the one accelerometer (i.e., axially). The parachute phase was more difficult to reconstruct for several of reasons. First, while the assumption was that the parachute was only influenced by drag, some side force would be created when the vehicle velocity (or parachute) is not aligned with the vehicle axis of revolution (the measurement direction for the axial accelerometer). Without lateral accelerations, off nominal conditions (such as wind gusts) are difficult to verify. Also, there are multiple possible solutions that can match the axial acceleration, but not satisfy other measured constraints (such as total descent time or altitude rate of change) due to the unknown amount of lateral (and thus total) acceleration sensed by the system. Second, the probe spent over two hours on the drogue parachute at terminal velocity (very little acceleration). Finally, the acceleration data collected had nearly +/- 0.1 m/s$^2$ of noise in the signal.

Figure 17 shows the comparison of accelerations from a simulation only run, accelerometer bias reconstruction, unbiased flight accelerometer data, and gravity acceleration during the drogue parachute phases. Since the parachute should be at or very near terminal velocity, the measured acceleration should equal the acceleration due to gravity. Note that the simulation-only run and gravity have nearly the same acceleration after about 4000 sec; whereas, the unbiased accelerations are notably below the gravity values. A reconstruction case was run to determine the bias required to bring the measured accelerations inline with the gravity. Figure 18 shows the bias solution determined from the reconstruction run. The biased accelerations are shown in Fig. 17. It appears that the accelerometer is biased about 0.022 m/s$^2$ during this long drogue parachute phase. An accelerometer bias of this magnitude (2200 µ-g) is unusually large and not anticipated for a space quality instrument, particularly since just prior to atmosphere entry the bias was determined to be about 23 µ-g, as mentioned earlier. This change in bias by a factor of about 100 means that either the events occurring during the EDL, or the environment at Titan can substantially modify navigation sensors, something of which future planners need to be aware.
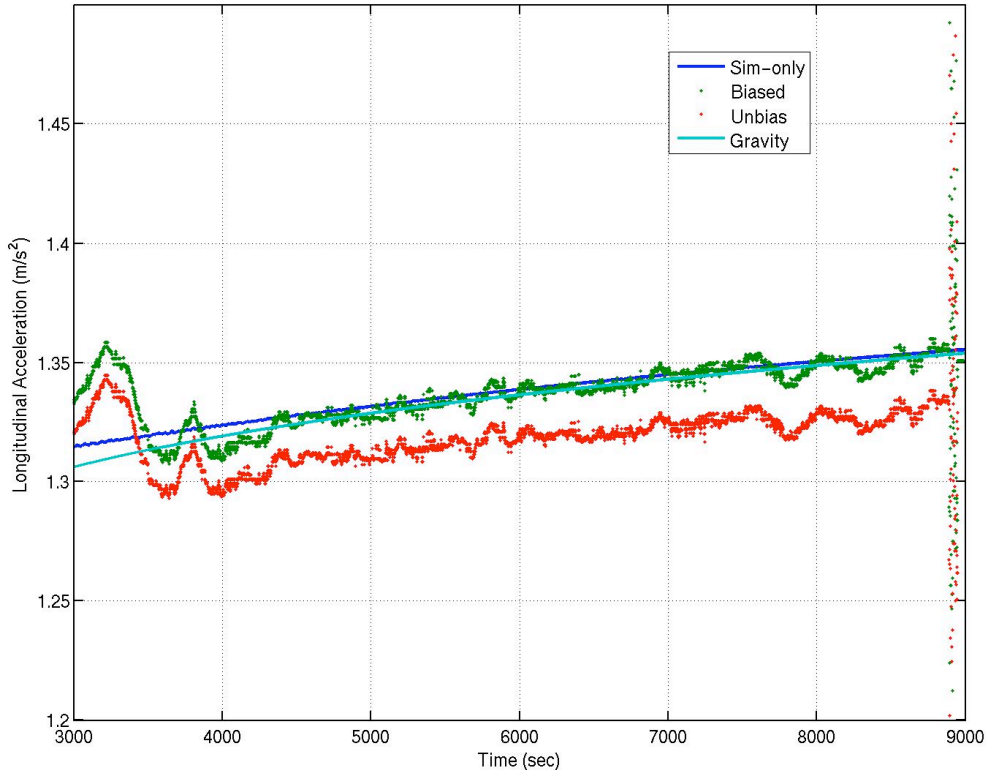
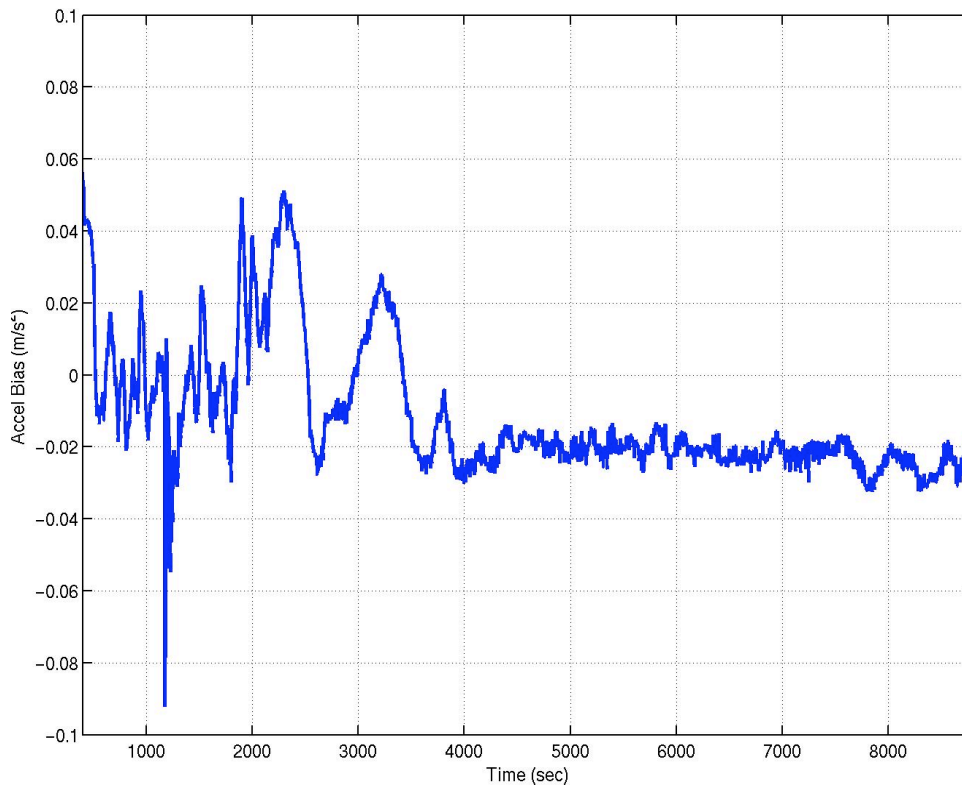Figure 17 Accelerations and Accelerometer Data in Drogue Phase



Figure 18  Estimated Bias to Measured Accelerometer Data

Also noted in Fig. 18 is a large variation in estimated bias prior to 4000 sec. This variation is also seen in the measured accelerations (see Fig. 5 between 2200 and 4000 sec) and would appear to be some (as yet undetermined) phenomenon that occurred to the probe. One possible explanation would be a wind shear, but no solutions thus far have been consistent across all measured data. That is, a solution can be found which matches the axial acceleration profile using vertical wind shears, however this solution provides altitude rates inconsistent with those derived from the pressure and temperature measurements and a shorter duration descent than was recorded from probe radio transmissions and surface impact measurements.  Thus, a bias prior to about 3800 sec was not established or used for solutions.

State (Position, Velocity) Estimate Runs

These trajectory reconstruction runs, focused on estimating the vehicle state (position and velocity) throughout the entire EDL trajectory, were done using the initial state determined from the Monte Carlo analyses as indicated above. The bias determined in the preceding section was also applied to these cases. The deceleration pulse during entry for this reconstructed trajectory is shown in Fig. 19. The region of maximum deceleration in this figure shows that while the reconstruction run captured the acceleration well, it did not overly adjust the state to meet the measurements.  The region just after parachute deploy also shows good agreement between the flight and reconstructed accelerations.
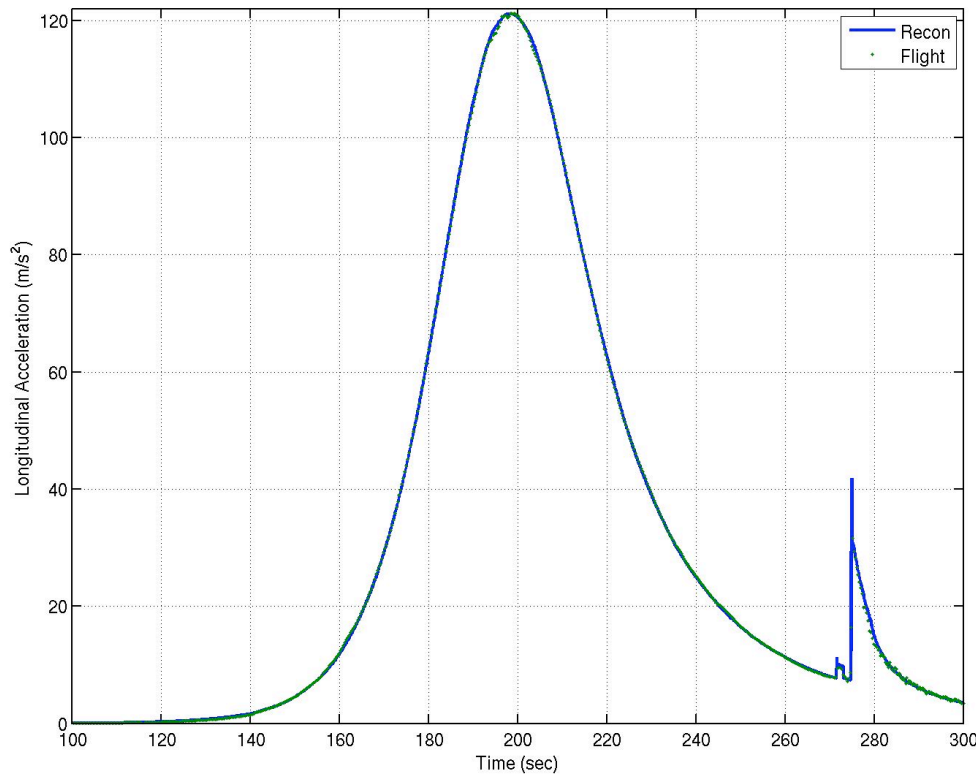


Figure 19.  Huygens Flight Data Compared to State Estimate Reconstruction Run– Entry Phase

Figures 20 and 21 focus on the flight data comparison at the end of the Main parachute and throughout the Drogue parachute phases. These figures illustrate the agreement between the flight axial accelerations and those generated using the reconstructed trajectory. The reconstructed trajectory data matches well through the fifteen minute Main parachute phase and through most of the Drogue phase. The curves separate slightly between 2000 and 2500 sec, but come back into agreement as time progresses. Note that the reconstruction case follows the biased accelerometer data as desired (see Fig. 21).
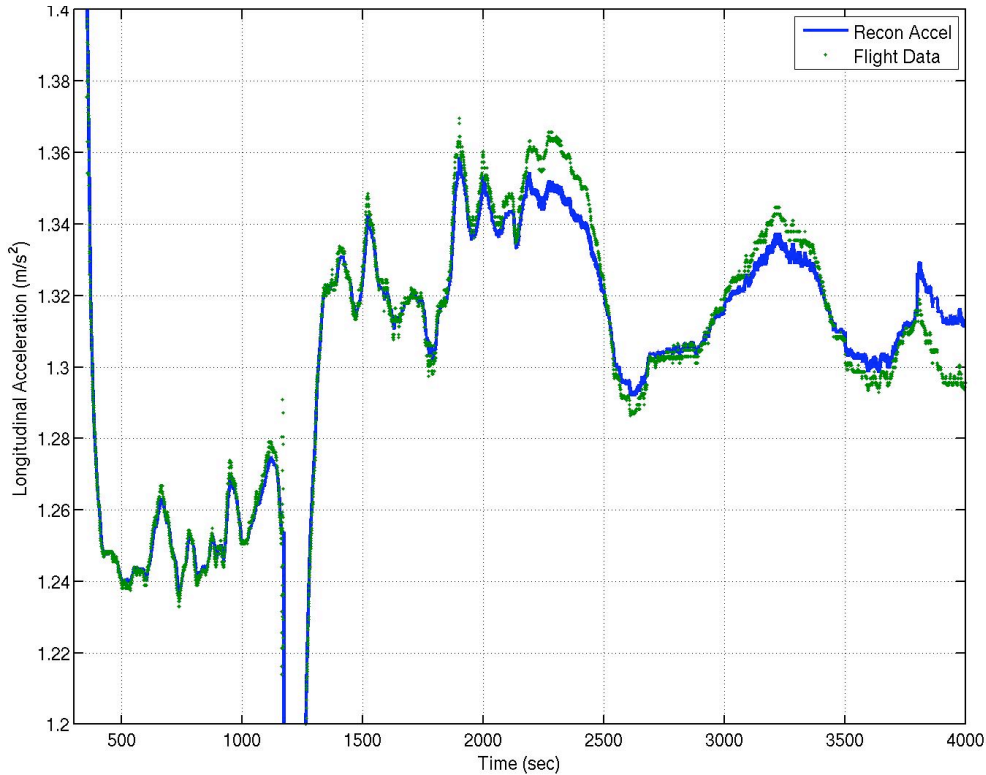


Figure 20. Comparison of Flight Data to State Estimate Reconstruction Run – Main and Drogue Parachute Phases
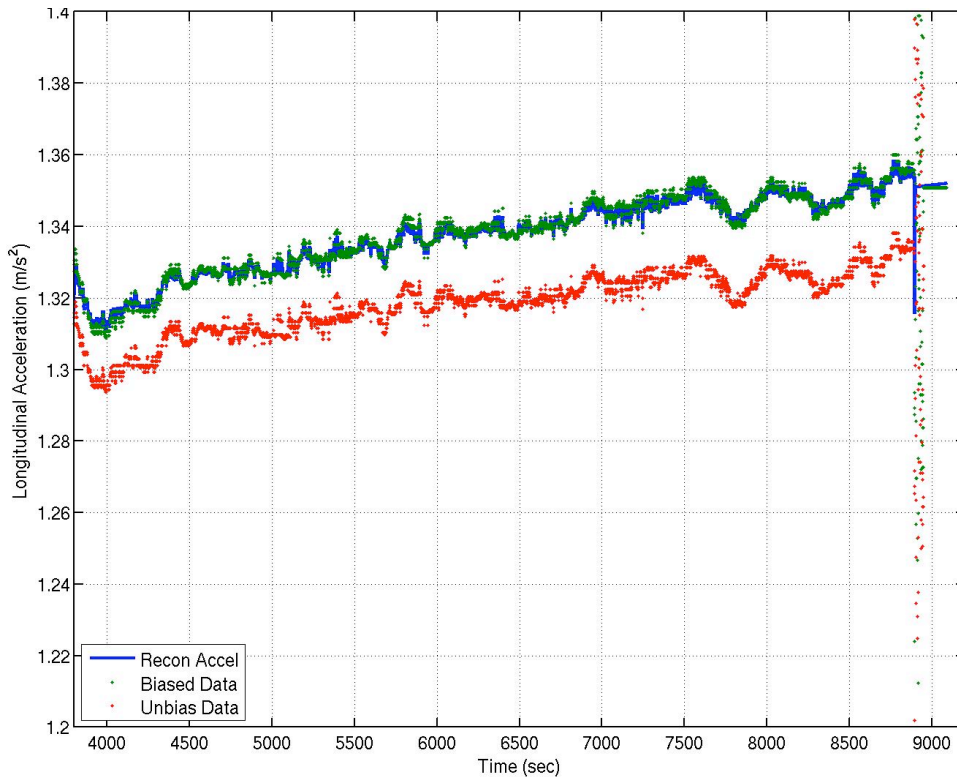
Figure 21. Comparison of Flight Data to State Estimate Reconstruction Run – Drogue Parachute Phase

A comparison of the altitude versus time for the reconstruction case and the radar altimetry data for unit A is included in Fig 12. As noted in the figure, the reconstruction case is slightly below the radar altimetry, by about 5 km, at the highest altitude but then reduces to less than 100 m by touchdown. A comparison of several reconstruction cases is shown in Fig. 22. As noted in this figure, all of the cases show a similar comparison to the radar data. This result would indicate that a scale factor should be applied to the radar data.
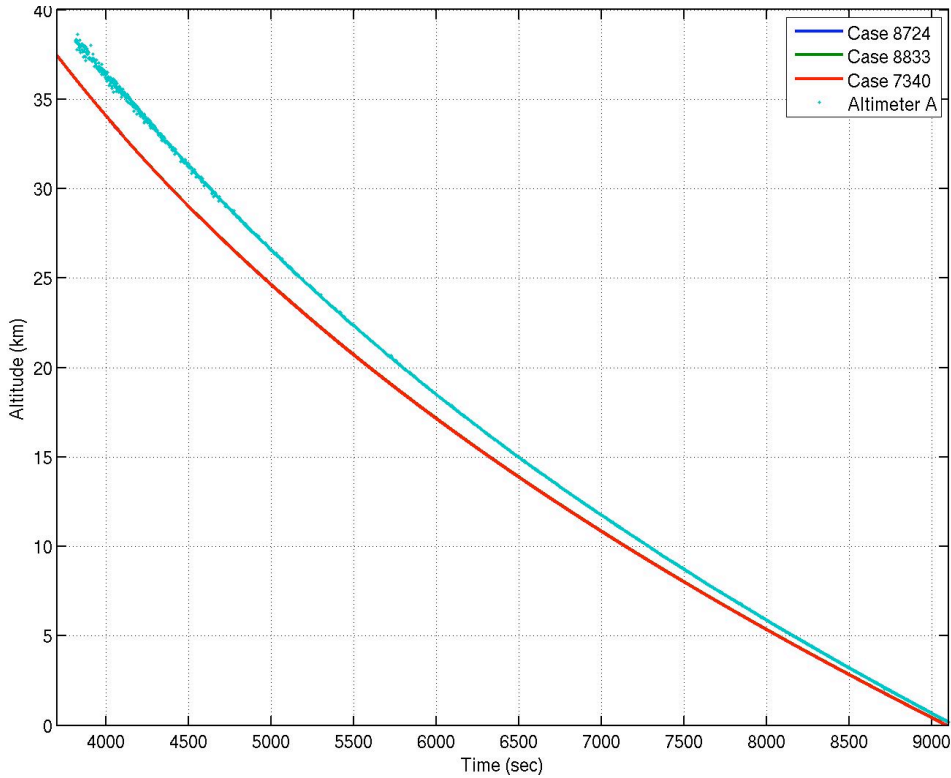
Figure 22. Altitude Profile for State Estimate of Several Cases –Radar Altimetry Comparison

Figure 23 shows the effect of a 0.93 scale factor on the radar data when compared to the same cases as shown in Fig. 22. This very good agreement between adjusted flight data and multiple reconstructed trajectories suggests that an adjustment of the radar data may be required. Alternatively, other possibilities exist that would also affect the radar measurements, namely probe tilt and radar electronics temperature sensitivity, but those possibilities were not considered this analysis.
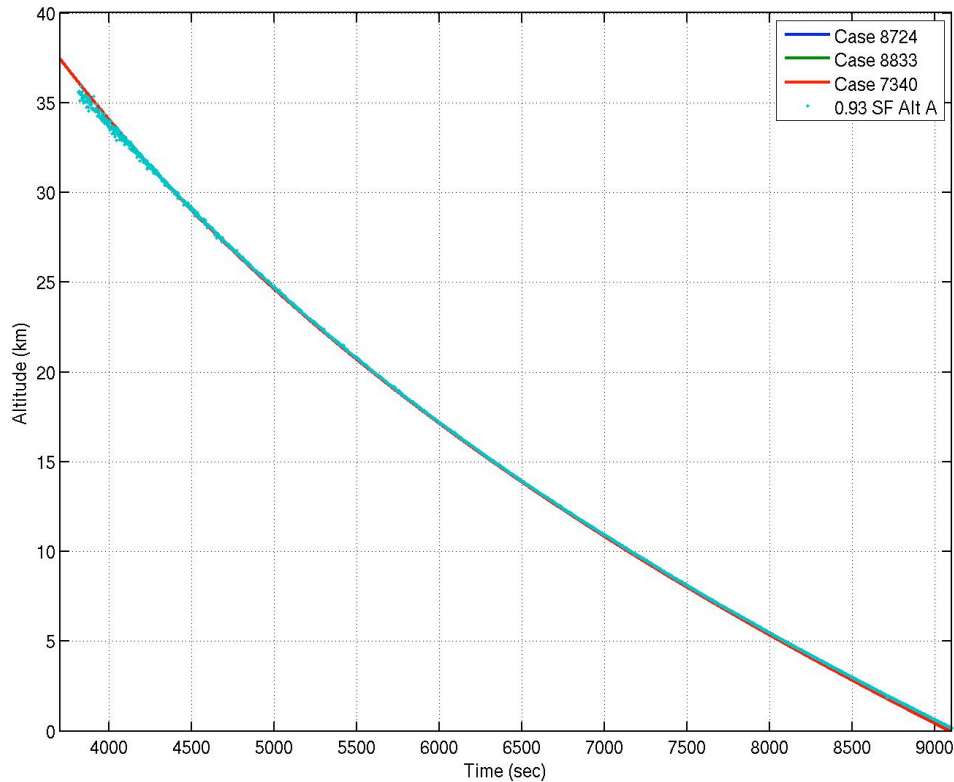
Figure 23. Altitude Profile for State Estimate of Several Cases–Radar Altimetry Scale Factor

## CONCLUSIONS

Trajectory reconstruction of the Huygens probe entry and descent at Titan was completed using two separate approaches: a traditional method and a POST2 simulation based method. Both reconstruction methods showed agreement with the DTWG and Carlo Bettanini generated altitude profiles that are in conflict with the altimetry flight data returned from both radars. A scale factor of about 0.93 would bring the radar measurements into compliance. Further analysis shows that the Titan-GRAM atmosphere model was within 1% of the reconstructed density below about 160 km altitude (or where the onboard pressure and temperature measurements began). A bias in the accelerometer measurements of around 0.022 $m/s^2$ after about 3800s from atmospheric interface was also suggested from the data analysis. Finally, an assessment of the entry aerodynamics model (generated prior to entry) showed that the variation in the aerodynamics as shown by the flight data was well within the 3-sigma bounds established by the aerodynamicists before entry.

## ACKNOWLEDGEMENTS

## REFERENCES

[1] Lebreton, J.-P., et al., "An overview of the descent and landing of the Huygens probe on Titan", *Nature*, Vol 438, 8 Dec 2005, pp 758-764.

[2] Lebreton, J.-P., and D. L. Matson (1997), "The Huygens Probe: Science, payload and mission overview", Space Science Reviews, Vol. 104, 2002, pp. 59-100.

[3] Kazeminejad, B., et al., "Huygens' Entry and Descent through Titan's Atmosphere – Methodology and Results of the Trajectory Reconstruction", *Planetary and Space Science*, in Press, 2007.

[4] Bird, M. K. et al., "The vertical profile of winds on Titan". *Nature*, Vol 438, 8 Dec 2005, pp 800-802.

[5] Fulchignoni, M. et al., "In situ measurements of the physical characteristics of Titan's environment", *Nature*, Vol 438, 8 Dec 2005, pp 785-791.

[6] Tomasko, M. G. et al. Rain, winds and haze during the Huygens probe's descent to Titan's surface." *Nature*, Vol 438, 8 Dec 2005, pp 765-778.

[8] Kazeminejad, B., *Methodology Development for the Reconstruction of the ESA Huygens Probe Entry and Descent Trajectory*. Ph.D. thesis, Karl-Franzens Univ., Graz, Austria, 2004.

[9] Folkner, W.M., et al., "Winds on Titan from ground-based tracking of the Huygens probe", *Journal of Geophysical Research*, Vol. 111, 2006,E07S02.

[10] NASA Engineering and Safety Center, "Assessment of the Cassini/Huygens Probe Entry, Descent and Landing (EDL) at Titan," NESC-RP-05-67, May 2005.

[11] Striepe, S.A., et al., "Program to Optimize Simulated Trajectories (POST II), Vol. II Utilization Manual." Version 1.1.6.G, January 2004, NASA Langley Research Center, Hampton, VA.

[12] Spencer, D.A., Blanchard, R.C., Braun, R.D., Kallemeyn, P.H., and Thurman, S.W., "Mars Pathfinder Entry, Descent, and Landing Reconstruction," *Journal of Spacecraft and Rockets*, Vol. 36, No. 3, 1999, pp. 357-366.

[13] Tolson, R.H., et al., "Application of Accelerometer Data to Mars Odyssey Aerobraking and Atmospheric Modeling," *Journal of Spacecraft and Rockets*, Vol. 42, No. 3, 2005, pp. 435-443.

[14] Witkowski, A., et al., "Mars Exploration Rover Parachute System Performance", AIAA Paper 2005-1605, 18th AIAA Aerodynamic Decelerator Systems Technology Conference and Seminar, Munich, Germany, May 2005.

[15] Spencer, D.A. , Braun, R.D., "Mars Pathfinder atmospheric entry - Trajectory design and dispersion analysis**,**" *Journal of Spacecraft and Rockets* (ISSN 0022-4650), Sept./Oct. 1996, vol. 33, no. 5, pp. 670-676.

[16] Desai, P.N., Schoenenberger, M., and Cheatwood, F.M., "Mars Exploration Rover Six-Degree-Of-Freedom Entry Trajectory Analysis," Paper AAS 03-642, AAS/AIAA Astrodynamics Specialists Conference, Big Sky, Montana, August 3-7, 2003.

[17] Desai, P.N., Lyons, D.T., "Entry, Descent, and Landing Operations Analysis for the Genesis Re-Entry Capsule," Paper AAS 05-121, 15th AAS/AIAA Space Flight Mechanics Conference, Copper Mountain, CO, January 23-27, 2005.

[18] Desai, P.N., Mitcheltree, R.A., and Cheatwood, F.M., "Entry Trajectory Issues for the Stardust Sample Return Capsule," International Symposium on Atmospheric Reentry Vehicles and Systems, March 16-18, 1999, Arcachon, France.

[19] Striepe, S.A., Way, D.W., Dwyer, A.M., and Balaram, J., "Mars Smart Lander Simulations for Entry, Descent, and Landing," AIAA Paper 2002-4412, AIAA Atmospheric Flight Mechanics Conference, Monterey, CA, August 2002.

[20] Justus, C.G., et al, "Connecting atmospheric science and atmospheric models for aerocapture at Titan and the outer planets," *Planetary and Space Science. Surfaces and Atmospheres of the Outer Planets, Their Satellites and Ring Systems* (ISSN 0032-0633), April 2005, Volume 53, no. 5, pp. 601-605.

[21] Gelb, A. (ed.). *Applied Optimal Estimation*, MIT Press, Cambridge, MA, 1974.

[22] Brown, R.G, and Hwang, P.Y.C., *Introduction to Random Signals and Applied Kalman Filtering*, John Wiley and Sons, New York, NY, 1992.